

Spin-polarized reflection in a two-dimensional electron system

Hong Chen, J. J. Heremans,^{a)} J. A. Peters, and A. O. Govorov

Department of Physics and Astronomy, and The Nanoscale and Quantum Phenomena Institute, Ohio University, Athens, Ohio 45701

N. Goel, S. J. Chung, and M. B. Santos

Department of Physics and Astronomy, and Center for Semiconductor Physics in Nanostructures, The University of Oklahoma, Norman, Oklahoma 73019

(Received 7 September 2004; accepted 9 November 2004; published online 14 January 2005)

We present a method to create spin-polarized beams of ballistic electrons in a two-dimensional electron system in the presence of spin-orbit interaction. Scattering of a spin-unpolarized injected beam from a lithographic barrier leads to the creation of two fully spin-polarized side beams, in addition to an unpolarized specularly reflected beam. Experimental magnetotransport data on InSb/InAlSb heterostructures demonstrate the spin-polarized reflection in a mesoscopic geometry. © 2005 American Institute of Physics. [DOI: 10.1063/1.1849413]

The spin of electrons and holes in semiconductor heterostructures has attracted much recent interest, as a factor to realize new spin-based electronic device concepts,¹ and for its potential in realizing quantum computational schemes.² In heterostructures, spin can manifest itself through spin-orbit interaction (SOI), leading to a spin-splitting in energy levels, and hence in the Fermi contours. Two SOI mechanisms typically predominate: the Rashba mechanism, originating from the inversion asymmetry of the heterostructure confining potential, and the Dresselhaus mechanism, from the bulk inversion asymmetry.³ Recent studies have often regarded SOI as deleterious, since it can lead to short spin-coherence times. If the mean free path in the heterostructure is longer than the lateral device dimensions, charge transport in the device occurs ballistically, i.e., the preponderant scattering events involve the device boundaries.⁴ If in such mesoscopic devices the spin-coherence length is longer than the mean free path, then SOI, together with the device geometry, can be exploited for spin manipulation, and for the preparation of spin-polarized carrier states. Theoretical studies have explored the effect of SOI on one-dimensional mesoscopic transport, and on vertical transport through heterostructures.⁵ Here we present a method to create spin-polarized beams of ballistic electrons by utilizing elastic scattering off a barrier in a straightforward geometry, and present experimental results verifying the realization of the method. As illustrated in Fig. 1(a), a beam of two-dimensional electrons in a heterostructure is injected toward a barrier. Both energy and the momentum parallel to the barrier are conserved during the scattering event off the barrier [Fig. 1(b)]. In previous ballistic transverse magnetic focusing experiments,⁴ energy and momentum conservation led to specular reflection. However, if the Fermi contours are spin-split, spin-flip scattering events result in different reflection angles for different spin polarizations [Figs. 1(b) and 1(c)]. Indeed, in the presence of SOI, scattering off the barrier can lead to spin-flip events, whereby a carrier can be scattered into the other spin subband. The interaction with the barrier gives rise to three reflection angles, hence three beams: two spin-polarized side

beams and one unpolarized specular beam [Figs. 1(b) and 1(c)]. The reflected beams can then be captured through suitably positioned apertures [Fig. 1(a)]. The multibeam reflection process can be utilized to create spin-polarized electron populations, without the use of ferromagnetic contacts.⁶

Figure 1(d) shows the sample geometry. Equilateral triangles of inside dimensions 3.0 μm feature apertures, of conducting widths of ~0.3 μm, on two sides, while the left-hand side forms the scattering barrier. Several triangles are measured in parallel.⁷ The triangles were wet etched into n-type InSb/InAlSb heterostructures after electron beam lithography. The gentle wet-etching procedure affords highly reflecting barriers in III-V heterostructures.⁴ Carriers enter the geometry from the top, travel ballistically to the left barrier, reflect off the latter, and exit through the bottom aperture. The total distance, including the reflection, between the apertures, amounts to 2.6 μm. The heterostructures were grown by molecular beam epitaxy on (100) GaAs substrates, and consisted of a 20-nm-wide InSb well, with the two-dimensional electron system (2DES), flanked by

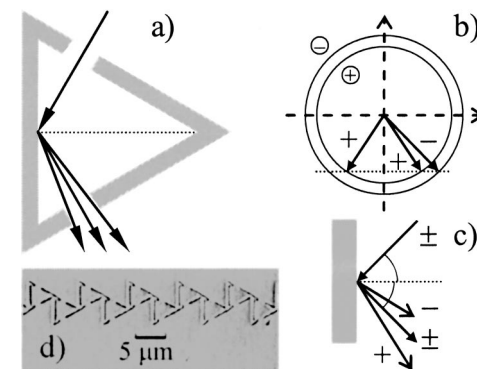


FIG. 1. (a) Schematic of the geometry. Electrons are injected at the upper aperture, scatter from the left barrier, and are collected at the lower aperture. A perpendicular magnetic field B allows the trajectories to sweep the lower exit aperture. Trajectories are indicated for $B=0$. (b) Geometrical interpretation of the spin-polarized scattering event, with incident and reflected wave vectors at the Fermi surface (for clarity only scattering of incident + spin states is depicted). Energy and the momentum parallel to the barrier are conserved. (c) The scattering geometry, with spin states denoted + and -. Spin-flip events at the barrier lead two spin-polarized side beams and one unpolarized specular beam. (d) Image of sample S_1 .

^{a)}Author to whom correspondence should be addressed; electronic mail: heremans@ohio.edu

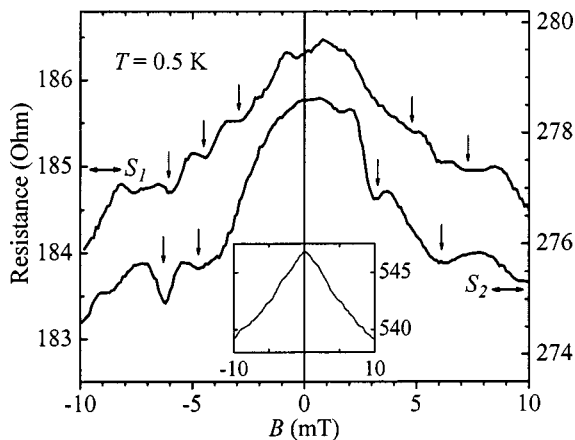


FIG. 2. The four-contact resistance of the triangular structures S_1 and S_2 , vs the perpendicular applied magnetic field B . The arrows indicate the values of B where beam cutoffs occur. Inset: Magnetoresistance of an antidot lattice fabricated on the same heterostructure (antidot diameter $0.4\ \mu\text{m}$, periodicity $0.8\ \mu\text{m}$), showing, for comparison, a featureless negative magnetoresistance background. Geometrical resonances appear at higher B (not shown).

$\text{In}_{0.91}\text{Al}_{0.09}\text{Sb}$ barrier layers.⁸ Electrons are provided by Si δ -doped layers on both sides of the well, separated from the 2DES by 30 nm spacers. A third Si doped layer lies close to the heterostructure surface. All measurements were performed at 0.5 K, and at this temperature, a density $N_S=2.6\times 10^{11}\ \text{cm}^{-2}$ and a mobility of $150\ 000\ \text{cm}^2/\text{V s}$ provide a mean free path of $\sim 1.3\ \mu\text{m}$. Although shorter than the distance between the two apertures in Fig. 1, this mean free path is sufficiently long to ensure observation of a signal due to a ballistic trajectory. Indeed, the cutoff of the signal at the mean free path is not abrupt, but rather is characterized by a gradual decay of the signal amplitude.^{4,7}

In our measurements, a current is drawn between the two apertures [Fig. 1(a)], and the resulting voltage drop is measured as a function of a magnetic field applied perpendicular to the plane of the 2DES. In the semiclassical limit, the magnetic field B serves to slightly deflect the ballistic carriers from linear trajectories, and thus to sweep the trajectories over the exit aperture. Varying B in either direction causes the three reflected beams to be sequentially cut off, by either side of the exit aperture. Each cutoff results in a stepwise rise in the resistance measured over the structure. In the experimental realization the cutoffs will not be sharp, since we expect an angular spread at the injection aperture. However, the angular spread is sufficiently narrowed by the previously observed collimating effect in mesoscopic apertures,⁹ to allow separate observation of the effects of the centroids of the three, partially overlapping, beams. Figure 2 contains experimental data for two separate samples (S_1 and S_2), plotted as the four-contact resistance measured over the triangular structures, versus applied B . For sample S_1 , five minima are indicated at low B , superimposed on a negative magnetoresistance weak-localization background. The five minima are interpreted to result from the stepwise increase in resistance as B is varied, added to the negative magnetoresistance background. We also note here that the wet-etching process results in uncertainty in the structure's dimensions, and that therefore a nonzero B may have to be applied to center the three beams on the exit aperture. Hence, the five minima are not centered around $B=0$. The number of cutoffs and their occurrence with B is dependent on the geometry resulting from the lithographic process. For instance, sample S_2 under-

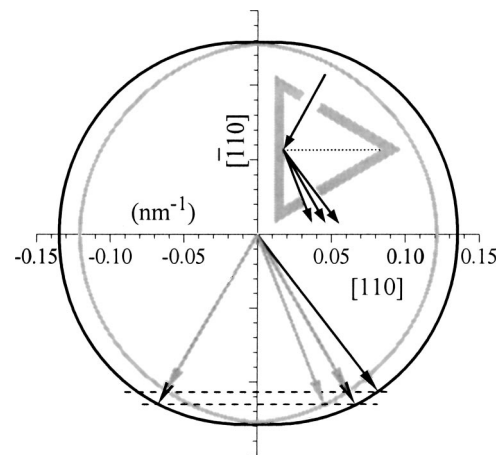


FIG. 3. Calculated Fermi contours at the density of the experiment, with the incoming and reflected wave vectors. Inset: orientation of the triangles.

went a deeper wet-etch, resulting in narrower apertures (also higher resistance values), and wider barriers. These geometrical differences lead to the occurrence of magnetoresistance features at different B as compared to sample S_1 . For sample S_2 , four magnetoresistance minima associated with the spin-dependent reflection phenomenon are indicated. In the following paragraph, we determine the correlation between the data in Fig. 2 and the three-beam reflection process in our experimental geometry.

Experimental values for the SOI parameters in InSb-based heterostructures have only recently been accessed by optical measurements, and the experimental data confirm SOI larger than in most other III-V materials.¹⁰ Separate evaluation of the Rashba and Dresselhaus contributions¹¹ has not yet been performed on InSb/InAlSb heterostructures. Hence, to ascertain the correlation between the data in Fig. 2 and the spin-dependent reflection process, we have calculated the Fermi contours in the plane of the InSb quantum well at the density of the measurement, including the nonparabolic dispersion in InSb.¹² The contours in Fig. 3 were obtained using a Rashba parameter $\alpha=1.0\times 10^{-11}\ \text{eV m}$ and a Dresselhaus parameter $\eta=7.6\times 10^{-28}\ \text{eV m}^3$.¹² There is ambiguity concerning α , since α depends on the average electric field in the well, which is not directly known. However, the value we use not only yields good agreement with the data, but moreover corresponds to an average electric field in the well of $1.9\times 10^6\ \text{V/m}$, an acceptable value for the 2DES density. The Dresselhaus term leads to anisotropy, and appears to dominate the Rashba term by a factor ~ 2 in our InSb quantum wells. The calculated anisotropic spin splitting ranges from 0.65 meV in the $[1\bar{1}0]$ direction to ~ 5.9 meV around the $[110]$ direction (at the average Fermi wave vector $k_F=\sqrt{2\pi N_S}$). The average spin splitting value approaches the value of 3 meV obtained from the optical measurements on similar InSb/InAlSb heterostructures.¹⁰ The inset of Fig. 3 depicts the orientation of the device within the Fermi contours. At an incident angle of 30° to the barrier, reflection angles of 21° , 30° , and 38° can be inferred from the Fermi contours. We have utilized these reflection angles in a semiclassical geometrical model that analytically calculates the position of the magnetoresistance minima, assuming circular cyclotron orbits (clearly an approximation, but within the experimental uncertainty). The magnetoresistance features for S_1 and S_2 agree with the model if we as-

sume for S_1 a conducting aperture width of $0.3 \mu\text{m}$, and for S_2 a conducting aperture width of $0.2 \mu\text{m}$, along with an additional rightward shift of $0.06 \mu\text{m}$ of the reflection barrier. The shift necessary for S_2 corresponds to an effectively thicker barrier, in agreement with the deeper and wider etched trench for this sample. The model also indicates that equal spacing in B is not expected for the magnetoresistance features, due to the curvature of the semiclassical orbits (the minima for $B < 0$ are more closely spaced than for $B > 0$). The consistency between the data in Fig. 2 and the Fermi contours in Fig. 3, all using expected experimental values, supports the observation of the spin-dependent reflection process.

It is noticed that a critical incident angle exists, below which the higher-energy spin subband cannot be accessed by scattering from the lower-energy subband. The critical angle can be found by tracing a horizontal tangent to the inner Fermi contour (referring to Fig. 3) toward the outer Fermi contour. This incident angle gives rise to a wave traveling in the direction of the barrier but evanescent perpendicularly to the barrier. Detection and capture of this evanescent (and spin-polarized) wave, although not performed in our present experiment, may prove useful in spin-electronics applications as well.

Concerning the negative magnetoresistance background, we have consistently observed only a weak-localization peak in mesoscopic geometries fabricated in the InSb/InAlSb heterostructure, in contrast to the antilocalization signature observed in GaAs or InAs based 2DESS.¹³ Another example of a weak-localization peak in a mesoscopic geometry is shown in the inset in Fig. 2, namely the resistance versus applied perpendicular B , measured over an antidot lattice fabricated on the same heterostructure.¹⁴ The absence of antilocalization is not surprising in InSb. Antilocalization requires the Dyakonov-Perel' spin scattering mechanism to dominate, leading to a randomization of the spin precession process due to a weak SOI.¹³ Yet, due to large spin splitting in InSb, the impurity broadening is less than the spin-splitting, invalidating the conditions for Dyakonov-Perel' scattering and antilocalization ($\hbar/\tau \approx 0.5 \text{ meV}$, smaller than the average spin-splitting of $\sim 3 \text{ meV}$, where τ is the scattering time from the mobility mean free path). The dominant spin-scattering mechanism in InSb at low temperature is likely the Elliott-Yafet mechanism.¹⁵ An estimate of the spin-scattering time τ_s in the InSb/InAlSb heterostructures yields $\tau_s \approx 20\tau$. The estimate demonstrates that spin scattering is unlikely to occur within a mean free path, and that hence in our geometry the dominant spin-flip event is provided by the lithographic barrier.

Ballistic transport in triangular geometries has been investigated previously,¹⁶ with apertures positioned in the center of one side and at the triangle apex. A rich magnetoresistance spectrum was observed due to semiclassical and quantum dynamics of resonant orbits interior to the triangles. To ascertain if our observed magnetoresistance originates from similar dynamics, we calculated the semiclassical orbits at varying B for our geometry. Orbit indeed exist which in analogy with the previous work will result in magnetoresistance features. However, those orbits occur outside the range of B used in this experiment. We also note that the observed

magnetotransport features are unlikely to result from universal conductance fluctuations. Indeed, the resistance is measured over ten triangles in parallel, and hence universal conductance fluctuations, which are sensitive to the microscopic potential landscape of each individual triangle, will be averaged out.

In conclusion, we demonstrate experimentally spin-polarized reflection off a barrier in an InSb/InAlSb heterostructure. We show that the spin-orbit coupling leads to different reflection angles for different spin polarizations. The spin-polarized beams resulting from the interaction with the barrier can be utilized toward various spin electronics or quantum computational realizations.

J.J.H. acknowledges support from NSF Grant No. DMR-0094055 and M.B.S. from NSF Grant Nos. DMR-0080054 and DMR-0209371.

- ¹Y. Ohno, D. K. Young, B. Beschoten, F. Matsukura, H. Ohno, and D. D. Awschalom, Nature (London) **402**, 790 (1999).
- ²D. Loss and D. P. DiVincenzo, Phys. Rev. A **57**, 120 (1998).
- ³Y. A. Bychkov and E. I. Rashba, J. Phys. C **17**, 6039 (1984); G. F. Dresselhaus, Phys. Rev. **100**, 580 (1955).
- ⁴J. Spector, H. L. Stormer, K. W. Baldwin, L. N. Pfeiffer, and K. W. West, Appl. Phys. Lett. **56**, 967 (1990); J. J. Heremans, M. B. Santos, and M. Shayegan, *ibid.* **61**, 1652 (1992); J. J. Heremans, S. von Molnár, D. D. Awschalom, and A. C. Gossard, *ibid.* **74**, 1281 (1999).
- ⁵S. Datta and B. Das, Appl. Phys. Lett. **56**, 665 (1990); F. Mireles and G. Kirczenow, Phys. Rev. B **64**, 024426 (2001); X. F. Wang, P. Vasilopoulos, and F. M. Peeters, *ibid.* **65**, 165217 (2002).
- ⁶G. Schmidt, D. Ferrand, L. W. Molenkamp, A. T. Filip, and B. J. van Wees, Phys. Rev. B **62**, R4790 (2000); D. Grundler, *ibid.* **63**, 161307 (2001).
- ⁷K. Nakamura, D. C. Tsui, F. Nihey, H. Toyoshima, and T. Itoh, Appl. Phys. Lett. **56**, 385 (1990); F. Nihey, K. Nakamura, M. Kuzuhara, N. Samoto, and T. Itoh, *ibid.* **57**, 1218 (1990).
- ⁸K. J. Goldammer, W. K. Liu, G. A. Khodaparast, S. C. Lindstrom, M. B. Johnson, R. E. Doezena, and M. B. Santos, J. Vac. Sci. Technol. B **16**, 1367 (1998); K. J. Goldammer, S. J. Chung, W. K. Liu, M. B. Santos, J. L. Hicks, S. Raymond, and S. Q. Murphy, J. Cryst. Growth **201/202**, 753 (1999).
- ⁹L. W. Molenkamp, A. A. M. Staring, C. W. J. Beenakker, R. Eppenga, C. E. Timmering, J. G. Williamson, C. J. P. M. Harmans, and C. T. Foxon, Phys. Rev. B **41**, 1274 (1990).
- ¹⁰G. Khodaparast, R. C. Meyer, X. H. Zhang, T. Kasturiarachchi, R. E. Doezena, S. J. Chung, N. Goel, M. B. Santos, and Y. J. Wang, Physica E (Amsterdam) **20**, 386 (2004).
- ¹¹S. D. Ganichev, V. V. Bel'kov, L. E. Golub, E. L. Ivchenko, P. Schneider, S. Giglberger, J. Eroms, J. De Boeck, G. Borghs, W. Wegscheider, D. Weiss, and W. Prettl, Phys. Rev. Lett. **92**, 256601 (2004); Y. Kato, R. C. Myers, A. C. Gossard, and D. D. Awschalom, Nature (London) **427**, 50 (2004).
- ¹²R. Winkler, *Spin-orbit Coupling Effects in Two-Dimensional Electron and Hole Systems*, Springer Tracts Mod. Phys. Vol. 191 (Springer, Berlin, 2003).
- ¹³P. D. Dresselhaus, C. M. A. Papavassiliou, R. G. Wheeler, and R. N. Sacks, Phys. Rev. Lett. **68**, 106 (1991); T. Koga, J. Nitta, T. Akazaki, and H. Takayanagi, *ibid.* **89**, 046801 (2002); J. B. Miller, D. M. Zumbühl, C. M. Marcus, Y. B. Lyanda-Geller, D. Goldhaber-Gordon, K. Campman, and A. C. Gossard, *ibid.* **90**, 076807 (2003).
- ¹⁴H. Chen, J. J. Heremans, J. A. Peters, N. Goel, S. J. Chung, and M. B. Santos, Appl. Phys. Lett. **84**, 5380 (2004).
- ¹⁵P. Murzyn, C. R. Pidgeon, P. J. Phillips, J.-P. Wells, N. T. Gordon, T. Ashley, J. H. Jefferson, T. M. Burke, J. Giess, M. Merrick, B. N. Murdin, and C. D. Maxley, Phys. Rev. B **67**, 235202 (2003).
- ¹⁶L. Christensson, H. Linke, P. Omling, P. E. Lindelof, I. V. Zozoulenko, and K.-F. Berggren, Phys. Rev. B **57**, 12306 (1998).